

Ball Bearing Analysis with the ORBIS Tool

Jacob D. Halpin*

Abstract

Ball bearing design is critical to the success of aerospace mechanisms. Key bearing performance parameters, such as load capability, stiffness, torque, and life all depend on accurate determination of the internal load distribution. Hence, a good analytical bearing tool that provides both comprehensive capabilities and reliable results becomes a significant asset to the engineer. This paper introduces the ORBIS bearing tool. A discussion of key modeling assumptions and a technical overview is provided. Numerous validation studies and case studies using the ORBIS tool are presented. All results suggest the ORBIS code closely correlates to predictions on bearing internal load distributions, stiffness, deflection and stresses.

Introduction

ORBIS was first released to the public in 2008 and has been actively maintained and enhanced since. The program was developed to modernize the state-of-the-art for bearing codes. Most prior industry standard tools came from the MS-DOS era and required a flat-file type input deck for operation. While these codes pioneered the analytical bearing industry they required a fairly steep learning curve to operate proficiently. With the advent of 64-bit processors in modern computer technology, support for MS-DOS has declined rapidly leaving software programmers with the burden to update their codes. Unfortunately, many developers of the early bearing tools are no longer around to maintain their codes.

The development approach for ORBIS began with selection of the Java programming language for its foundation. Java was initially selected because it runs on a virtual machine that is supported by most computer platforms (i.e., Windows, Mac OS, Unix). Also, the widespread popularity of Java over the internet gave confidence that it would be actively supported for many years to come. Some additional fringe benefits of the Java language that proved particularly useful during the development stages were its object-oriented programming environment and support of multi-threaded processing.

The core bearing model used within ORBIS is based on A. B. Jones' mathematical theory of rolling element bearings [1]; herein referred to as the Jones model. This model provides a nonlinear solution to an entire system of bearings and has been the industry standard for many decades. The primary handicap to the Jones model is its inherent fixed ring assumption. This assumption is generally not tolerable for modern aerospace bearing designs, particularly those that utilize thin section bearings. ORBIS addresses this by including ring compliance algorithms into the core solver. These algorithms determine ring strain during the mounting, preloading, and thermal expansion stages of the solver, thereby greatly improving model accuracy. A more thorough discussion on key bearing modeling assumptions is provided herein.

To validate the ORBIS code a multi-tiered approach is taken. First, the core solver is compared against the A. B. Jones High Speed Ball and Roller Bearing Analysis Program. This comparison study includes twenty-nine different configurations and results such as maximum mean Hertzian contact stresses, bearing row displacements, row reaction forces, and row stiffness components are evaluated. Since these cases must use a fixed ring assumption to match the A. B. Jones program, the next validation step focuses on the ring compliance algorithms. In this study, Alan Leveille's codes BRGS10 and BRGS14 are compared in a case study that was jointly run by Brian Gore from Aerospace Corporation and Steve Koss from Naval Research

* Halpin Engineering LLC, Torrance, CA

Laboratories. The study compares the resolved mounted preload state on a hard preloaded duplex pair of bearings for variations to the bearing fits, contact angles, curvature, temperature and free preload.

The final section presents case studies, based on real bearing analyses found in a literature search, where published results are compared with ORBIS predictions. The first case study is from the 22nd Aerospace Mechanisms Symposia proceedings titled “Two Gimbal Bearing Case Studies: Some Lessons Learned” by S. H. Loewenthal. The second case study is from NASA/TP-2014-217906, titled “Analysis of Space Station Centrifuge Rotor Bearing Systems: A Case Study” by J. V. Poplawski, S. H. Loewenthal, F. B. Oswald, E. V. Zaretski, W. Morales, and K. W. Street.

Technical Model Overview

ORBIS uses numerical techniques to solve the nonlinear elastic behavior of the user-defined system of one or more bearing rows. The model considers each ball-to-race contact for all bearing rows defined in the system, resulting in complete knowledge of the element load distributions and their raceway attitudes. A solution to the system is achieved when the sum of all bearing row reaction forces is sufficiently close to the external applied forces (system equilibrium).

The system model follows the same process necessary to assemble a rotational system: initial conditions are defined, the bearings are fit into the assembly, preload is applied to the bearings, and external loading is finally applied to the mounted and preloaded bearing system. The parameters describing relative ring displacements and internal clearance changes are tracked at each step of the process; ultimately leading to the final state of the bearing system.

Since bearings typically operate with very small internal clearances, it is important to consider the effects of boundary conditions on the races when establishing the mounted state of the bearing system. ORBIS implements a compliance model based on classical thick ring theories to determine the final mounted and preloaded state of the bearing system. The compliance model is also used for assessing thermal strains. Once all mounting, preloading and thermal strains have been considered, the traditional fixed ring theories, as developed by Jones, are applied to assess effects due to external loading.

The compliance model makes a key assumption that in the local vicinity of the bearing, the housing, shaft and bearing rings can be expressed with a series of nested rings. Thick ring theory assumes the representative rings have uniform constant wall thickness and all deflections remain within the linear elastic region of the material. Since the groove side of a bearing race clearly has a non-constant cross section, an equivalent diameter has been developed to represent bearing rings. The equivalence model is shown in (1) and (2), and has been correlated to detailed finite element models. A key benefit to the equivalence model is that it is based on the geometry defining the raceway depth and therefore can account for the general class of raceways. The compliance algorithms also track various sudden changes in the boundary conditions of each nested ring; such as when the fit between a bearing outer diameter (O.D.) and housing inner diameter (I.D.) transitions from clearance to interference due to preload expansion or thermal expansion.

$$D_{IR} = d_{IR_{race}} + 0.68(h_l + h_d) - \frac{2h_l}{d_{IR_{race}}}(h_l - h_d) \quad (1)$$

$$D_{OR} = d_{OR_{race}} - 0.68(h_l + h_d) + \frac{2h_l}{d_{OR_{race}}}(h_l - h_d) \quad (2)$$

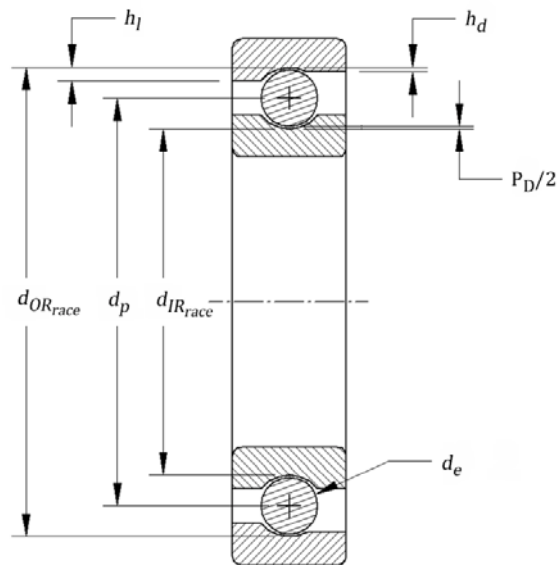


Figure 1. Bearing nomenclature for equivalent raceway diameter

Capabilities and Features

Brief overview of ORBIS

The ORBIS main graphical interface is shown in Figure 2. This interface is used to configure/setup the bearing system to be analyzed. ORBIS implements a database approach for definition of key common elements of the analysis, thereby making the setup, and subsequent attainment of results, a fairly quick process. Database features are provided for definition of bearings, materials and lubricants. Once these elements have been defined within the database, the user only needs to assign them to their system from the main interface.

Another noteworthy feature of the main interface is the system sketch (shown in the upper-right quadrant of the interface). This sketch provides a useful means for checking that the setup is as intended. Within the sketch is a drawing of all assigned rows along with their associated contact angle orientation. The bearing rows are labeled with their database name and coordinate position along the shaft. All assigned load points are also included with their defined coordinate positions. Additionally, rows that float on a preload spring are identified with a spring symbol adjacent to the bearing row.

Analytical results are displayed in a separate output window as shown in Figure 3. In addition to displaying tabulated text for the complete set of results, the window contains features to help recognize common results quickly. At the top of the window is a quick reference summary table of maximum values for mean stress, truncation, mounted preload and torque at each bearing row. The bottom region of the results window contains a control panel that allows the user to filter which results to display. Another feature, which is illustrated in the figure, is that all elements with stresses exceeding a predefined threshold are highlighted in red. Additionally, any element found to have truncation is always highlighted.

A more thorough description of the ORBIS software can be found at [2].

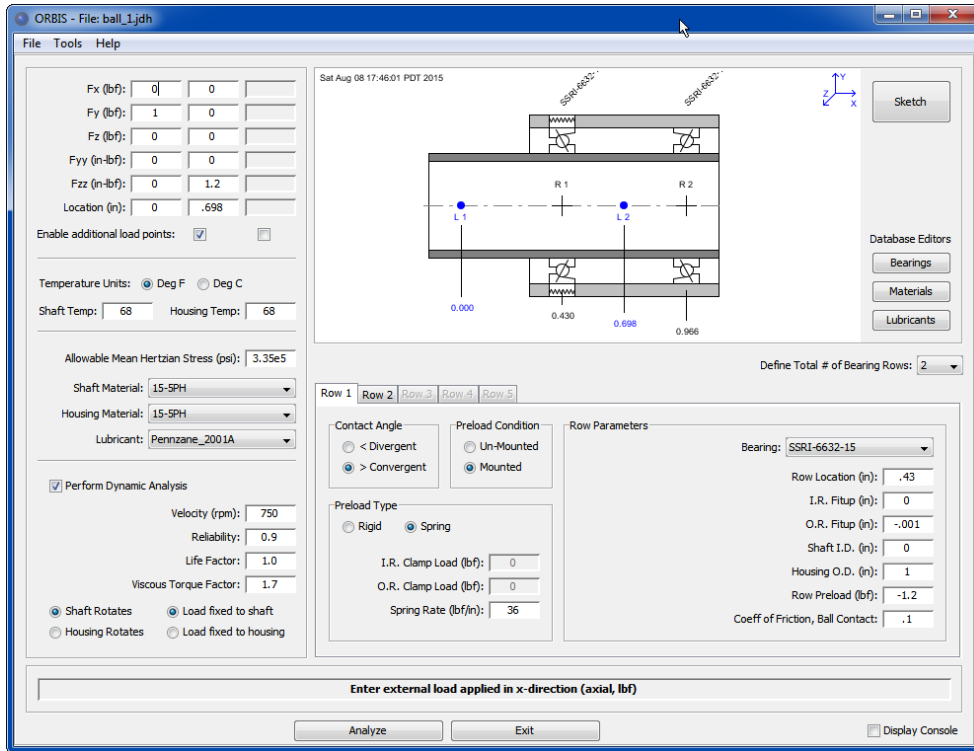


Figure 2. ORBIS main graphical interface

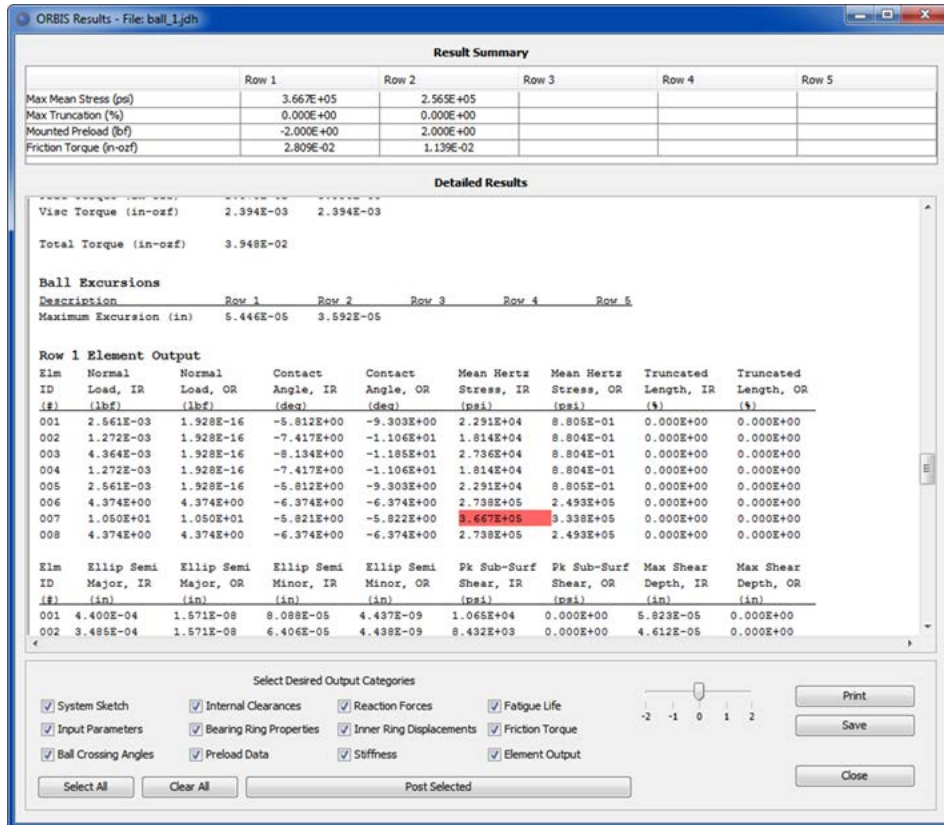


Figure 3. Result output window

Key Analytical Considerations

Mechanisms that implement rolling-element bearings typically rely on certain performance parameters from the bearings. The most common parameters are load capability, stiffness, torque, and operational life. As it turns out, all of these parameters are dependent on the internal load distributions—meaning normal loads and associated contact angles—within each bearing defined in the system. Given accurate loaded contact angles of each element within a system, Hertzian contact mechanics provide the elliptical contact areas that are the basis for solving stresses, stiffness, primary torque components, and the fatigue life. Hence, the importance of accurately predicting the internal load distributions of a system of bearings should be foremost.

A point often overlooked in the analysis of bearings, which is particularly true for aerospace mechanisms due to their extremely high launch load environment, is that external loads are typically derived by analytical means, such as finite element modeling, and thus the bearing element stiffness is required as an input to the finite element model. This creates a circular process where the bearing stiffness is needed in order to predict the loads on the bearings. Additional complications arise due to the fact that finite element models require a linear stiffness yet bearing stiffness is nonlinear with load. Typically, the best that can be done here is to determine a linear approximation of the bearing stiffness in the vicinity of the load recovery. This may require more than one iteration to establish.

Abstract models of real systems are based on assumptions of the phenomena modeled and it is therefore prudent to review such assumptions. Let's first discuss the inherent assumptions of the mathematical theories derived by A. B. Jones. The Jones model can be summarized as follows. Each raceway's center of curvature is represented with a fixed diameter circle. The outer raceway circles are fixed in space and a local coordinate frame is attached at the center of the inner raceway circles. Inner raceway displacements, which are relative to the fixed outer rings, create differences to the normal approach between the inner and outer circles. The location of the ball center, relative to the fixed outer raceways, and solved at each ball station, is determined by ensuring the ball is in quasi-static equilibrium. A Newton-Raphson search routine then iterates on displacements to the moveable coordinate inner rings. Given the normal approach of the ball center relative to each raceway, classical Hertzian contact analysis is utilized to determine normal loads and elliptical contact areas at each raceway contact point. The vector sum of all ball loads then provides the resultant force reacting on the shaft for a given set of inner ring displacements. Complete bearing equilibrium is achieved when the shaft reaction forces are equal, or sufficiently close, and opposite to the externally applied loads.

The Jones method, which is a very elegant derivation, does rely on the assumption that raceway circles maintain a fixed radius (a.k.a. fixed ring assumption). Should the raceways expand or contract it would change the normal approach to the ball center and could have a profound effect to the internal load distribution. Most traditional bearing materials are intentionally selected to be very hard and stiff and typical normal approach dimensions of the contacting bodies are on the order of 5 micrometers (0.0002 inch). This implies very small changes to the normal approach can have a profound effect on contact angles and normal loads. Such changes should therefore be included in the predictive model to enhance accuracies.

Items such as interference fitting, ring clamping, preloading and thermal expansions will all effect the bearing ring diameters. Most of which, if not all, are inherent in every mechanism containing rolling-element bearings. Before continuing our discussion on key model assumptions lets illustrate some common mounting influences with an example. Figure 4 illustrates a duplex pair of angular contact bearings that are oriented back-to-back. Although not shown in the figure we shall assume the bearings are hard preloaded by some means (perhaps a clamp plate or jam nut). It is well known that such systems as this can be quite sensitive to the mating fits of the bearing. Also, since the bearings are mounted in structure with a higher coefficient of thermal expansion than the bearing material (e.g., aluminum shaft and housing versus 440C bearings), we expect that temperature excursions will also affect the internal load distribution of the mounted bearings.

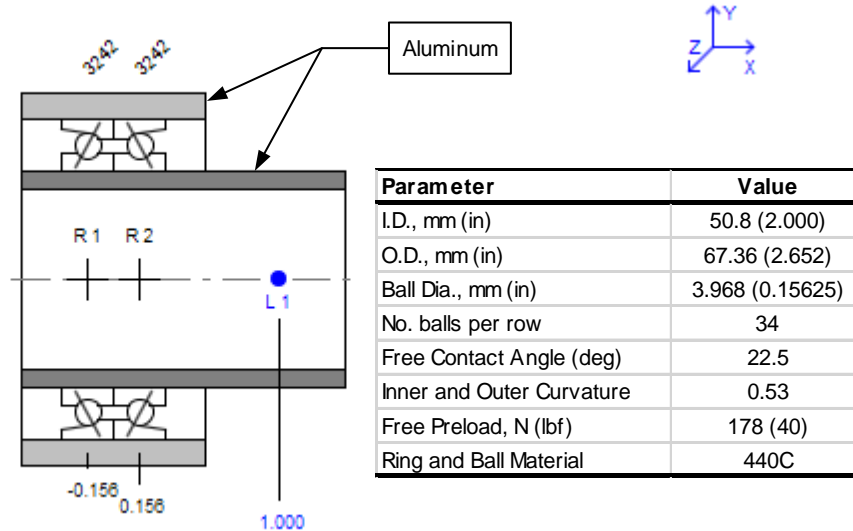


Figure 4. Example problem

Using the sensitivity utility in ORBIS allows us to perform parametric studies of inner ring fits and bulk system temperature. This utility takes the user defined system and allows perturbations to an input variable, such as inner ring fit up or bulk system temperature, to be plotted against selected output variables, such as mounted preload and maximum stress.

Figure 5 shows two pairs of plots illustrating the effects of inner ring fit up and bulk temperature of the system on the mounted preload and mean Hertzian stress of the bearings. Figures 5a & 5b illustrate that small amounts of interference at the inner diameter of the bearing cause a rapid increase in the mounted preload. This occurs because the expansion of the inner ring reduces the free contact angle of the bearing; thereby increasing the manufactured preload gap, also referred to as the ring stick-out, between the abutting inner ring faces. With a hard-preloaded system, this gap is forced closed and the balls must react the increased strain.

Figures 5c & 5d show the effects of the aluminum expansion rates on the bearings. The plots illustrate that as the temperature is either increased or decreased from ambient the mounted preload and stress will increase. Initial fits for this example are line-to-line on the shaft and $5\ \mu\text{m}$ (0.0002 in) clearance on the housing. Note that the influence to cold temperature is more pronounced than when the system is heated above ambient. At first glance, this may not seem intuitive since both the shaft and housing are made from aluminum. Hence, as you heat the system above ambient the inner ring fit gets tighter and the outer ring fit gets looser and, adversely, as you cool the system the outer ring fit gets tighter while the inner ring fit gets looser. In either case one ring of the bearing is driven by its boundary condition, however for the bearing to react preload the ball must have equal loads at both raceways. Therefore, the rate of preloading will be a function of the loose ring's hoop stiffness. Since the inner ring has a higher hoop stiffness than the outer ring it will react loads quicker and thus the cold case is more sensitive. Another contribution to why the cold case is worse is the fact that the diameter of the outer ring is larger than the inner ring and, for a given temperature delta from ambient, the magnitude of diametral change for the outer ring will slightly exceed that of the inner ring.

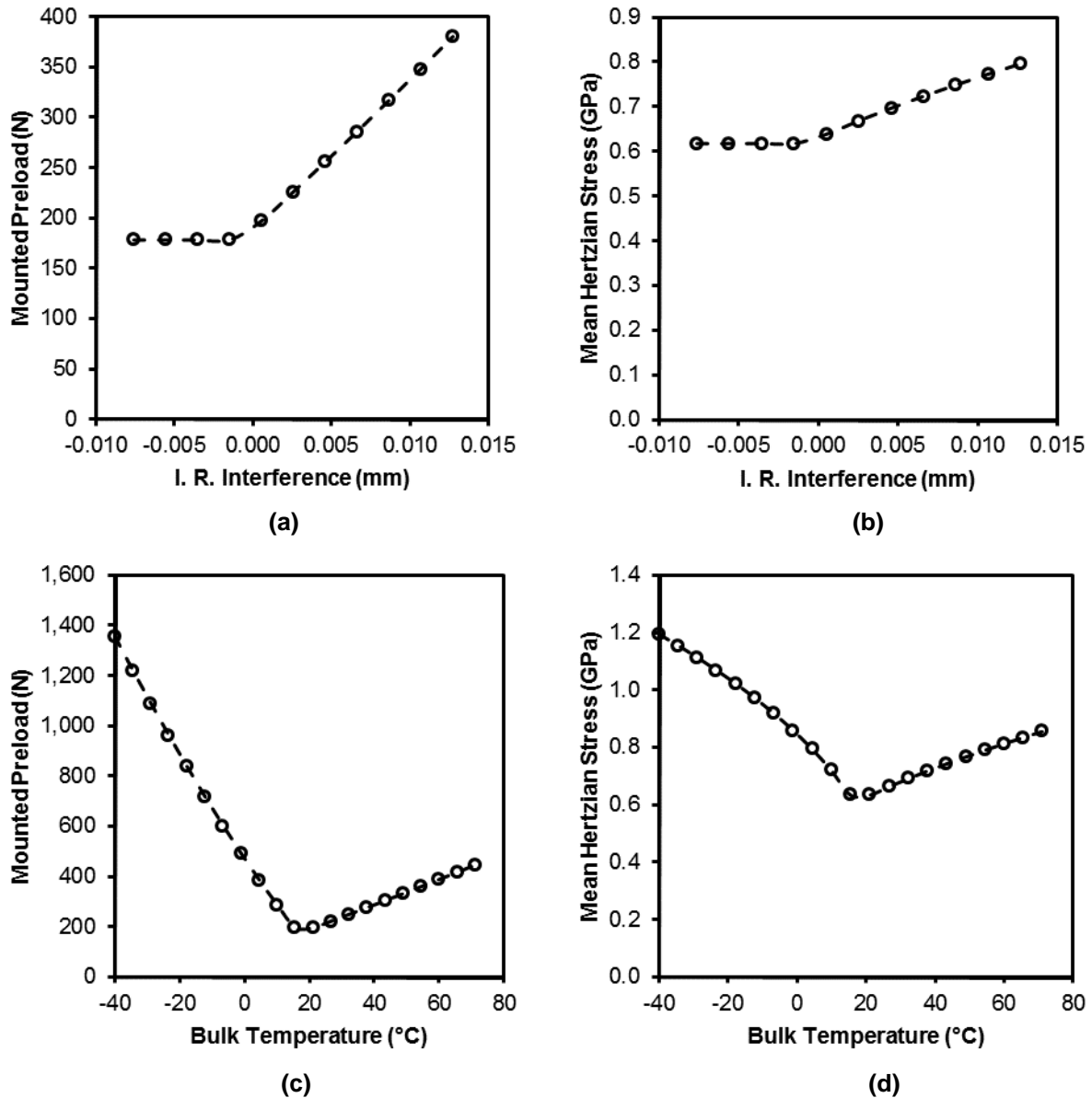


Figure 5. Effects of inner ring fit up on (a) mounted preload and (b) mean Hertzian stress and effects of shaft and housing bulk temperature on (c) mounted preload and (d) max mean Hertzian stress

One other noteworthy modeling assumption, which is inherent in the Jones model, is that the contact area between the rolling elements and raceways are always fully contained. When the contact ellipse is not fully contained, it is said to be truncated. A truncated contact area will invalidate the reported stress but also incurs errors to the resolved internal load distribution since the contact stiffness is a function of the contact area. There are some simple methods to de-rate the stress for truncated elements but not the stiffness. Hence, it becomes important to, at a minimum, know when a system has truncation.

Model Validation

Core Jones Model

Since ORBIS is based on theories published by A.B. Jones, validation of the core solver can be achieved by comparing identical analysis cases with the A. B. Jones High Speed Ball and Roller Bearing Analysis Program. Numerous test cases were designed to demonstrate that ORBIS maintains accuracy for wide variety of different system geometry. Key results tracked for comparison included maximum mean Hertzian contact stresses, bearing row displacements, row reaction forces, and row stiffness components. These result parameters validate that the nonlinear elastic system solver is correctly determining the internal load distributions and Hertzian contact mechanics for the bearing system.

Twenty-nine test cases were developed for this comparison and are shown in Table 2. The characteristic system consisted of a back-to-back pair of bearings with a single central load point. Note that contact angles, raceway curvatures and material properties were held constant for all test cases. These parameters will be more thoroughly studied in the flexible ring validation cases discussed later. Independent axial, radial and moment loading was studied to verify principal load component accuracy. Combined, or simultaneous loading (all 5 directions), was also studied and included variations in system preload, bearing size, number of balls, ball diameter and bearing row separation.

As shown in Table 1, which summarizes the percent differences between ORBIS and Jones software for all twenty-nine test cases, ORBIS results correlate to the A.B. Jones program within a fraction of one percent. These differences are deemed insignificant and likely relate to either differences in convergence criteria for the Newton-Raphson solver or rounding errors between the two programs (note that ORBIS maintains 64-bit floating point precision while it is believed that the Jones code might only hold 16-bit precision). Figure 6 depicts the Hertzian stress comparisons for each of the test cases.

Table 1. Comparison of all results

Comparison Parameter	% Difference		
	Min	Mean	Max
Bearing Row Stiffness Components	-0.1%	0.0%	0.2%
Inner Ring Deflections	-0.3%	0.1%	0.6%
Bearing Row Reaction Forces	-0.2%	0.0%	0.8%
Max Mean Hertzian Contact Stress	-0.5%	-0.3%	0.0%

Table 2. Test Case Parameters

Case	Bore (mm)	O.D. (mm)	# Balls	Ball Dia. (mm)	Row Span (mm)	Preload (N)	F_x (N)	F_y (N)	F_z (N)	M_y (Nm)	M_z (Nm)
1	12.7	19.05	21	1.59	38.10	89	89	89	89	2.26	2.26
2	19.05	25.4	30	1.59	50.8	178	178	178	178	4.52	4.52
3	25.4	34.93	28	2.38	69.85	267	267	267	267	226	226
4	50.8	66.68	34	3.97	133.35	356	445	890	890	452	452
5	76.2	92.08	50	3.97	184.15	445	890	1779	1779	904	904
6	101.6	114.3	80	3.18	228.6	667	1334	3559	3559	1695	1695
7	127	165.1	36	9.53	330.2	890	1779	4448	4448	2825	2825
8	152.4	190.5	42	9.53	381	1112	2669	8896	8896	5085	5085
9	127	165.1	36	9.53	254	890	-	-	-	-	-
10	127	165.1	36	9.53	254	890	2224	-	-	-	-
11	127	165.1	36	9.53	254	890	4448	-	-	-	-
12	127	165.1	36	9.53	254	890	8896	-	-	-	-
13	127	165.1	36	9.53	254	890	1.78E4	-	-	-	-
14	127	165.1	36	9.53	254	890	3.56E4	-	-	-	-
15	127	165.1	36	9.53	254	890	7.12E4	267	-	-	-
16	127	165.1	36	9.53	254	890	-	2224	-	-	-
17	127	165.1	36	9.53	254	890	-	4448	-	-	-
18	127	165.1	36	9.53	254	890	-	8896	-	-	-
19	127	165.1	36	9.53	254	890	-	1.78E4	-	-	-
20	127	165.1	36	9.53	254	890	-	3.56E4	-	-	-
21	127	165.1	36	9.53	254	890	-	7.12E4	-	-	-
22	127	165.1	36	9.53	254	890	-	-	-	113	-
23	127	165.1	36	9.53	254	890	-	-	-	226	-
24	127	165.1	36	9.53	254	890	-	-	-	452	-
25	127	165.1	36	9.53	254	890	-	-	-	904	-
26	127	165.1	36	9.53	254	890	-	-	-	1808	-
27	127	165.1	36	9.53	254	890	-	-	-	3616	-
28	127	165.1	36	9.53	254	890	-	-	-	7232	-
29	127	165.1	36	9.53	254	890	-	-	-	14464	-

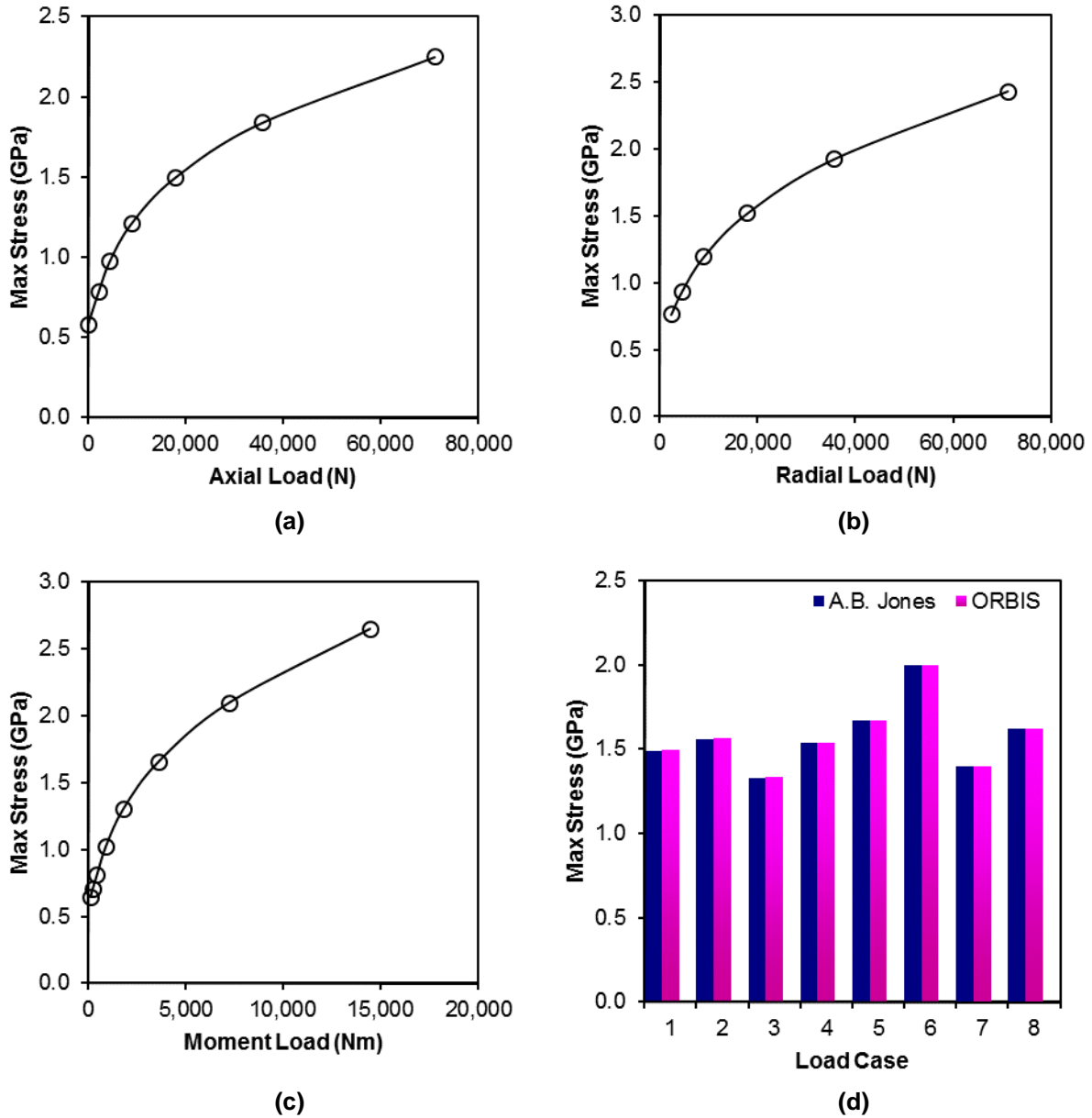


Figure 6. Comparison of maximum mean Hertzian contact stresses for various loading. ORBIS results denoted with circles and A. B. Jones results shown with solid line. (a) shows axial loading, (b) shows radial loading, (c) shows moment loading and (d) shows 8 combined load cases.

Ring Compliance Model Validation

Since the ring compliance model is used to establish the mounted, or operating, conditions we shall first consider a simple duplex pair of bearings against a well-known code that contains both ring compliance and considers both thermal expansions and ring clamping. The configuration consists of a duplex pair of angular contact bearings oriented back-to-back with a hard preload. The shaft and housing are made from titanium and the bearing rings and balls are 440C. Variations of the free contact angle, raceway curvatures, shaft and housing temperatures, I.D. and O.D. fits, and pre-ground preload are studied. Comparison of the predicted mounted preload are made against two different versions of A. Leveille's code: BRGS10 and BRGS14.

Table 3 shows key setup parameters for the system that were fixed during the study. Table 4 shows the various run cases studied along with the resulting mounted preload condition from all three codes. As shown, ORBIS correlates much closer with BRGS14 than BRGS10. Average difference between ORBIS and BRGS14, for all cases considered, is within 5.3%. It is believed that the earlier version of Leveille's code (BRGS10) does not contain an account for ring clamping, which would explain why it predicts lower mounted preloads. It is not known how Leveille modeled the bearing ring stiffness, particularly the derivation of the equivalent diameter for the grooved side of the races. A common rule of thumb for ring influences is to take approximately 80% of the interference as internal clearance loss in the bearing. This method is not recommended as it assumes a fixed ratio of the stiffness between the boundary and bearing ring.

Table 3. Setup parameters for mounted preload study

Parameter	Value	Parameter	Value
Pitch Dia., mm (in)	171.45 (6.750)	Housing O.D., mm (in)	202.18 (7.960)
Ball Dia., mm (in)	9.525 (0.375)	Modulus of Elasticity, Rings & Balls, GPa (psi)	200 (2.90E+07)
No. Balls	42	Poisson's Ratio, Rings & Balls	0.28
Shoulder Height (h/d)	0.206	Coefficient of Thermal Expansion, Rings & Balls, 1/°C	1.02E-05
Dam Height (h/d)	0.011	Modulus of Elasticity, Shaft & Housing, GPa (psi)	112 (1.62E+07)
Row Width, mm (in)	19.05 (0.750)	Poisson's Ratio, Shaft & Housing	0.31
Row Straddle, mm (in)	19.05 (0.750)	Coefficient of Thermal Expansion, Shaft & Housing, 1/°C	8.82E-06
Shaft I.D., mm (in)	134.62 (5.300)		

Table 4. Mounted preload study results

Initial Conditions (Free)							Mounted Preload (N)		
Contact Angle (deg)	I.R. & O.R. Curvature	Shaft / Housing Temp (°C)	I.D. Clearance (mm)	O.D. Clearance (mm)	Clamping Force (N)	Ground Preload (N)	BRGS10	BRGS14	ORBIS V2.4.1
22.5	54.5	76/76	0.01397	0.01905	53378	5115	5538	6112	5858
		-10/-10					5373	5133	5084
							3327	3861	3643
20.0		66/76				4226	2300	2931	2718
22.5	55.0						2447	3051	2851
								2331	2954
25.0	54.0		0.02286	0.03048			2108	2785	2540
			0.00508	0.00762			2189	2264	2246
							2838	3318	3087

Case Studies

This first example is taken from the proceedings of the 22nd AMS [3]. Here, we focus on Loewenthal's first case study. The described design consists of a large thin section (12" (30.5-cm) O.D., 11" (27.9-cm) I.D. and 0.250" (6.35-mm) diameter balls) duplex pair of angular contact bearings, oriented face-to-face that is hard preloaded in beryllium structure. The bearing system must operate with fairly large radial thermal gradients. Loewenthal mentions that he found it more expedient to construct a special purpose bearing code to solve this class of problem. In his study, Loewenthal constructed a design plot to show maximum contact stresses versus the radial thermal gradient. Using the Sensitivity Utility within ORBIS and holding the outer race temperature fixed while varying the shaft temperature the maximum contact stresses were solved. These data were then exported from ORBIS for post processing and, as shown in Figure 7,

constructed as a function of gradient along with a few points from Loewenthal's plot. As shown, ORBIS correlates well with Loewenthal's predictions for most of the gradient spectrum considered (note: original units have been converted to SI in accordance with AMS policy). The biggest difference between the two predictions occurs at -20°F (-29°C) case, where ORBIS predicts about twice the stress. Note that this region of bearing stress is highly nonlinear because the contact area is approaching a theoretical point (near zero ball loads).

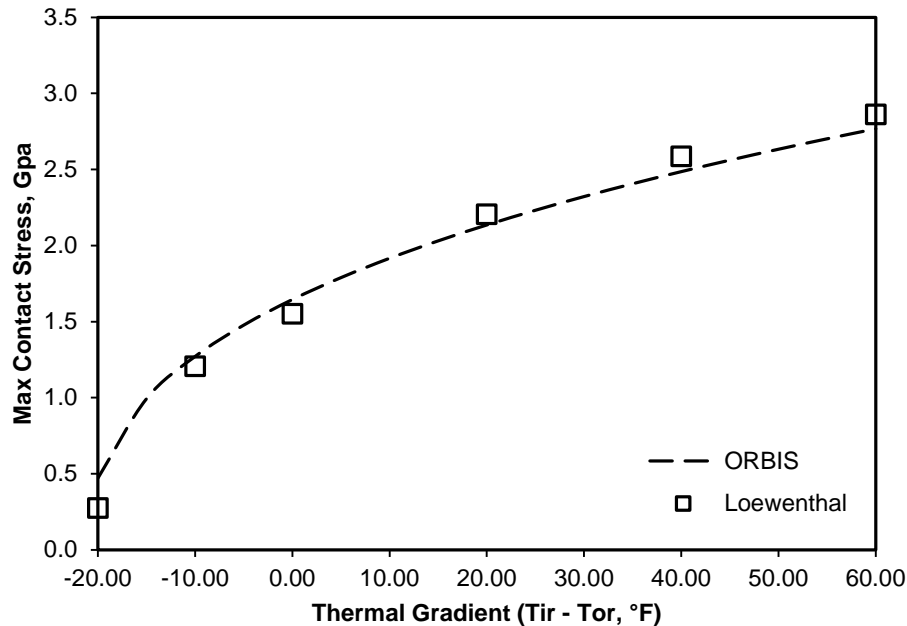


Figure 7. Comparison of thermal gradient stresses to Loewenthal's paper

The next example is from an analysis of the space station centrifuge rotor bearing system [4]. In this study, the rotor shaft assembly is analyzed for both bulk temperature loading and thermal gradients. The rotor shaft assembly is comprised of a three-bearing system: a duplex face-to-face pair and deep-groove (Conrad) bearing. The housing and shaft are aluminum 7075-T73 and all bearing rings and balls are 440C stainless. Figure 8 shows the cross section of the rotor shaft assembly. As shown, the system has a fairly large span (~600 mm) and preload springs are located on rows 2 and 3 (where row 1 is the leftmost row in the figure). Due to both the bearing span and fact that the housing and shaft are made from aluminum there are obvious concerns regarding how this bearing will react to both bulk temperature and temperature gradients.

Figure 8 shows the results from ORBIS plotted against the original publication. Here, we have chosen to plot only rows 2 and 3 because row 1 does not differ from row 2 appreciably (row 1 and 2 being the face-to-face pair). As shown, ORBIS matches very closely with the original author for both bulk temperature loading and temperature gradients. Row 3, which is the deep-groove bearing, clearly has the most sensitivity to temperature fluctuations. It should be noted that the ambient shaft fit for row 3 has a fairly profound effect on the contact angle and the publication only mentions a range, or tolerance, for this parameter. The results shown assumed this fit was at its minimum value (0.022 mm). Also, as shown in Figure 8 (right), row 3 has a maximum predicted contact angle that is approximately 2 degrees higher from the publication when the gradient is 20°C. All other points, which are located at both higher and lower gradients, have a much smaller deviation (less than 1° average). This one point appears a bit out of family compared with the other points.

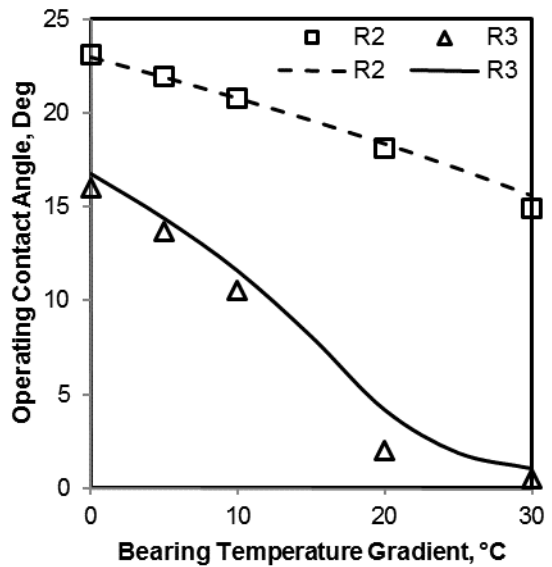
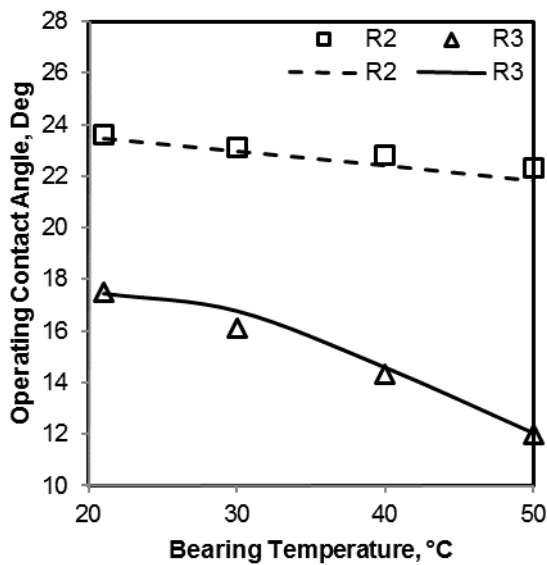
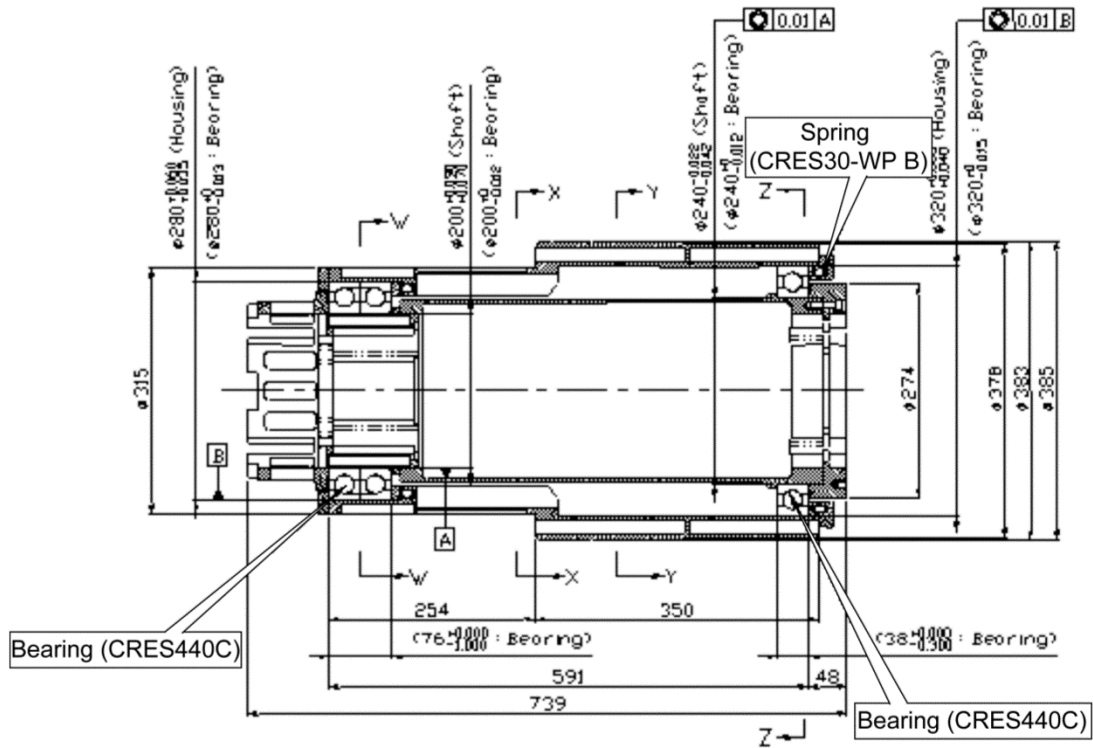


Figure 8. Main rotor assembly cross section (reference Figure 2 in [4]) and comparison of operating contact angle predictions. Left: rows 2 & 3 shown against bulk bearing temperature (reference Figure 3 in [4]). Right: rows 2 & 3 shown against bearing temperature gradient (reference Figure 5 in [4]).

Conclusion

Many aerospace designs contain bearing rings have been thinned down to minimize weight. They may also utilize dissimilar materials for the bearing support structure. Such systems require ring compliance considerations to accurately determine the internal load distribution of the bearings and, ultimately, the proper performance assessment of the bearings. The ORBIS software tool has been introduced and was developed to account for these effects. Various key technical analysis considerations, including relevant assumptions and a description of the compliant ring modeling, has been discussed. Numerous validation cases, including a few published bearing analysis studies, were performed and all results suggest the code closely correlates to other trusted predictions. In addition to providing reliable results, the tool offers a significant upgrade from the earlier MS-DOS based programs. Forethought has been taken to help ensure ORBIS will provide long-term dependability and robust compatibility with various computer operating systems and machine architectures by using the Java programming language. Moreover, ORBIS strives to eliminate many hand calculations often required with other programs and provides iterative design utilities that allow the user to quickly understand and assess the performance of their bearing system.

References

- [1] A. B. Jones, "The Mathematical Theory of Rolling-Element Bearings," in *Mechanical Design and Systems Handbook*, New York, McGraw-Hill, 1964.
- [2] J. D. Halpin, "Halpin Engineering - Software," 2016. [Online]. Available: <http://www.halpinengineeringllc.com/software>.
- [3] S. H. Loewenthal, "Two Gimbal Bearing Case Studies: Some Lessons Learned," in *22nd Aerospace Mechanisms Symposium*, Hampton, 1988.
- [4] J. V. Poplawski, S. H. Loewenthal, F. B. Oswald, E. V. Zaretski, W. Morales and K. W. Street, "NASA/TP-20142217906 Analysis of Space Station Centrifuge Rotor Bearing Systems: A Case Study," NASA, Cleveland, 2014.